

The ISW effect and the lack of large-angle CMB temperature correlations

Craig J. Copi^{1*}, Márcio O’Dwyer^{1,2†}, Glenn D. Starkman^{1,3‡}

¹*CERCA/Department of Physics/ISO, Case Western Reserve University, Cleveland, OH 44106-7079, USA*

²*The Capes Foundation, Ministry of Education of Brazil, Brasília DF 70359-970, Brazil*

³*Observatorio Nacional, Rio de Janeiro, RJ 20921-400, Brazil*

Accepted XXX. Received YYY; in original form ZZZ

ABSTRACT

It is by now well established that the magnitude of the two-point angular-correlation function of the cosmic microwave background temperature anisotropies is anomalously low for angular separations greater than about 60 degrees. Physics explanations of this anomaly typically focus on the properties of the Universe at the surface of last scattering, relying on the fact that large-angle temperature fluctuations are dominated by the Sachs-Wolfe effect (SW). However, these fluctuations also receive important contributions from the integrated Sachs-Wolfe effect (ISW) at both early (eISW) and late (ℓ ISW) times. Here we study the correlations in those large-angle temperature fluctuations and their relative contributions to $S_{1/2}$ – the standard measure of the correlations on large angular scales. We find that in the best-fitting Λ CDM cosmology, while the auto-correlation of the early contributions (SW plus eISW) dominates $S_{1/2}$, there are also significant contributions originating from cross-terms between the early and late contributions. In particular, realizations of Λ CDM with low $S_{1/2}$ are typically produced from a combination of somewhat low pure-early correlations and accidental cancellations among early-late correlations. We also find that if the pure ℓ ISW auto-correlations were the only contribution to $S_{1/2}$ in Λ CDM, then the p -value of the observed cut-sky $S_{1/2}$ would be unremarkable. This suggests that physical mechanisms operating only at or near the last scattering surface could explain the observed lack of large-angle correlations, though this is not the typical resolution within Λ CDM.

Key words: cosmic background radiation – large-scale structure of Universe.

1 INTRODUCTION

The temperature (T) and E -mode polarization fluctuations of the Cosmic Microwave Background (CMB) are widely regarded as one of the great successes of the standard cosmological model – inflationary Lambda Cold Dark Matter (Λ CDM). Even so, some anomalies, particularly on large angular scales, have been identified (for reviews of anomalies see Copi et al. 2010; Bennett et al. 2011; Planck Collaboration et al. 2015a; Schwarz et al. 2015). In this paper we focus on the first identified anomaly – the absence of two-point angular correlation in the CMB temperature maps for angular separations above approximately 60 degrees. While this was originally noticed in the *COBE-DMR* data (Hinshaw et al. 1996), it was first quantified by the *WMAP* team

in their first-year data release (Spergel et al. 2003) through a statistic, $S_{1/2}$, which we recall below. This $S_{1/2}$ statistic has been found to be anomalously low on the full reconstructed CMB sky and even more so on the cleanest part of the sky in all full-sky maps since the first-year *WMAP* Independent Linear Combination (ILC) map and including all CMB-dominated single-waveband maps (Copi et al. 2006, 2007, 2009, 2013a).

The lack of large-angle correlation in the temperature two-point angular correlation function could be a statistical fluke: our Universe could be a rare realization of the Λ CDM ensemble. Though we cannot probe other universes from the ensemble, this ‘fluke hypothesis’ can be tested (Hajian 2007; Dvorkin et al. 2008; Copi et al. 2013b; Yoho et al. 2014, 2015). Alternatively, the observed lack of large-angle correlation may be due to new physics, the simplest ideas involving modifications at the last scattering surface (LSS) of the CMB.

The dominant contribution to low- ℓ T power is the

* E-mail: cjc5@case.edu

† E-mail: marcio.odwyer@case.edu

‡ E-mail: glenn.starkman@case.edu

Sachs-Wolfe (SW) effect on the LSS – the effect on photon energy due to the difference between the Newtonian potential on the LSS and the potential at the observer. Much of the thought (so far unsuccessful) into how to explain the low- $S_{1/2}$ anomaly has therefore concentrated on eliminating large-angle correlations in the gravitational potential at last scattering. However, the integrated Sachs-Wolfe (ISW) effect – the result of photon propagation through a time-dependent potential – also contributes significantly at low- ℓ and large angles. This ISW effect itself can be divided into two major contributions – early-time (eISW), i.e. at high redshift, and late-time (ℓ ISW), i.e. at low redshift.

Presumably, any mechanism that de-correlated the gravitational potential on the LSS would eliminate correlations in both the SW and the eISW. The same is not true for the ℓ ISW. The obvious question then becomes – is it sufficient to eliminate correlations on or near the LSS in order to explain the smallness of $S_{1/2}$, or must whatever physics is at work also affect the ℓ ISW – either its auto-correlation or its cross-correlation with early-time physics?

We address this question by studying how the rare small- $S_{1/2}$ skies emerge by chance within Λ CDM. We do this by separately analysing contributions from early physics, late physics, and their correlations. We find that the typical means by which Λ CDM produces a rare realization with a low $S_{1/2}$ is by somewhat lowering the contribution from pure-early correlations and further reducing it through accidental cancellations due to early-late cross-correlations. Alternatively, we find evidence to suggest that postulating new physics at or near the LSS also has the potential to successfully explain the observed low value of $S_{1/2}$.

2 FORMALISM

Here we review the standard methods of describing temperature fluctuations and define the notation employed. The temperature two-point angular correlation function,

$$\mathcal{C}(\theta) \equiv \overline{T(\hat{\mathbf{e}}_1)T(\hat{\mathbf{e}}_2)}, \quad \hat{\mathbf{e}}_1 \cdot \hat{\mathbf{e}}_2 = \cos \theta, \quad (1)$$

is defined as the average over the sky (or some portion thereof) of the product between the temperature fluctuations $T(\hat{\mathbf{e}})$ in two directions separated by an angle θ . On a full sky, it contains the same information as the more familiar (in CMB physics) angular power spectrum, \mathcal{C}_ℓ , since

$$\mathcal{C}(\theta) = \sum_\ell \frac{2\ell + 1}{4\pi} \mathcal{C}_\ell P_\ell(\cos \theta), \quad (2)$$

where P_ℓ is the Legendre polynomial of order ℓ . Here \mathcal{C}_ℓ is given by

$$\mathcal{C}_\ell \equiv \frac{1}{2\ell + 1} \sum_m |a_{\ell m}|^2. \quad (3)$$

and the $a_{\ell m}$ are the coefficients of a spherical-harmonic expansion of the CMB temperature fluctuations

$$T(\hat{\mathbf{e}}) \equiv \sum_{\ell m} a_{\ell m} Y_{\ell m}(\hat{\mathbf{e}}). \quad (4)$$

Nominally, the lower limit of the sum in (2) should be $\ell_{\min} = 1$; however, since any intrinsic dipole is presumed to be overwhelmed by a much larger Doppler dipole from

which we are currently unable to separate it, all maps are monopole and dipole-subtracted, so $\ell_{\min} = 2$.

To quantify the observed lack of correlation above 60 degrees in their first year data, the *WMAP* team (Spergel et al. 2003) introduced the $S_{1/2}$ statistic,

$$S_{1/2} \equiv \int_{-1}^{1/2} [\mathcal{C}(\theta)]^2 d(\cos \theta). \quad (5)$$

This integral can more conveniently be rewritten as the sum

$$S_{1/2} = \sum_{\ell\ell'} \mathcal{C}_\ell I_{\ell\ell'} \mathcal{C}_{\ell'}, \quad (6)$$

where $I_{\ell\ell'}$ are elements of a known matrix (Copi et al. 2009). In the *WMAP* year one data, the p -value of $S_{1/2}$ in an ensemble of realizations of the best-fitting *WMAP* year one Λ CDM model was approximately 0.15 per cent. Since then, through all the *WMAP* and *Planck* data releases, with the various full-sky reconstruction algorithms and associated masks, that p -value has varied from about 0.03 per cent to 0.3 per cent for masks with this same cut-sky fraction. It is slightly higher (about 0.6 per cent) for the *Planck* Release-2 full-sky maps with the Common (UT78) mask, which only removes 22 per cent of the sky.

3 SEPARATING EARLY-TIME AND LATE-TIME EFFECTS

As remarked above, the CMB temperature power spectrum at low ℓ , or alternatively $\mathcal{C}(\theta)$ at large angles, is dominated by two contributions, the Sachs-Wolfe effect and the integrated Sachs-Wolfe effect. As also noted above, the early-time effects (SW and eISW) occur at high redshift, whereas the late-time effect (ℓ ISW) occurs at low redshift. These effects are thus well-separated in redshift, and we can think of these contributions to $\mathcal{C}(\theta > 60^\circ)$ as being divided into early-time and late-time physics. With this in mind, we can analyse early-time and late-time effects separately to determine how they combine to result in the small $S_{1/2}$ observed.

To separate early-time and late-time contributions we write the total spherical-harmonic decomposition coefficients as a sum of their early and late contributions,

$$a_{\ell m} = a_{\ell m}^e + a_{\ell m}^l, \quad (7)$$

where ‘e’ stands for early and ‘l’ for late. This separation corresponds to

$$\mathcal{C}_\ell = \mathcal{C}_\ell^{ee} + \mathcal{C}_\ell^{ll} + 2\mathcal{C}_\ell^{el}, \quad (8)$$

when written in terms of the power spectra. Here the superscripts represent two-point auto and cross-correlations between early-time and late-time anisotropies. With this separation the $S_{1/2}$ sum (6) can therefore be decomposed into six different contributions denoted by $S_{1/2}(X, Y)$ with

$$S_{1/2}(X, Y) \equiv \sum_{\ell\ell'} \mathcal{C}_\ell^X I_{\ell\ell'} \mathcal{C}_{\ell'}^Y \quad (9)$$

and $X, Y \in \{ee, ll, el\}$. The total $S_{1/2}$ is the sum over all of these contributions.

In Λ CDM, the early-time and late-time contributions to $a_{\ell m}$, the $a_{\ell m}^e$ and $a_{\ell m}^l$, are correlated Gaussian random variables with known correlations. Given values for the $a_{\ell m}$, either as realizations of the theory or extracted from cleaned

full-sky maps, the known theoretical correlations can be employed to generate constrained realizations of pairs of early and late skies from the Λ CDM ensemble. (See Appendix A for details.) From each realization, all the $S_{1/2}(X, Y)$ components can be calculated. To understand how the six $S_{1/2}(X, Y)$ components work together to reduce correlations on large scales (resulting in a low $S_{1/2}$) we generated realizations of early-sky and late-sky pairs imposing various constraints on the Λ CDM ensemble, as enumerated below.

3.1 Parameters

To generate realizations some choices must be made. Noting that the effects of interest occur on large angular scales, high resolution maps (or large multipole moments) are not required to capture the relevant information. For this reason, all calculations have been performed at a HEALPIX¹ resolution of $N_{\text{side}} = 64$ and with $\ell_{\text{max}} = 191$. Further, the best-fitting Λ CDM model parameters from *Planck* ($TT + \text{lowP} + \text{lensing}$) (Planck Collaboration et al. 2015b) were used along with the January 2015 version of the CAMB² code (Lewis et al. 2000) to generate the theory \mathcal{C}_ℓ along with the ℓ ISW only contribution ($z < 30$), \mathcal{C}_ℓ^l , and the early effects (SW+eISW), \mathcal{C}_ℓ^{ee} . The cross-correlation, \mathcal{C}_ℓ^{el} , is easily deduced from (8).

The mask and cleaned maps from *Planck* are provided at high resolution. These were degraded to $N_{\text{side}} = 64$ using the method employed in the *Planck* Release-2 analyses (Planck Collaboration et al. 2015a). Briefly, the $a_{\ell m}$ were extracted from the high resolution maps, scaled by the ratio of window functions between the new low resolution and original high resolution, and finally synthesized into a low resolution map. For degrading masks the additional step of setting all pixels with values less than 0.9 to zero, and all others to one, is performed.

Unless otherwise stated, all $S_{1/2}$ values are calculated from skies masked by the *Planck* Release-2 Common mask (degraded as described above) and with the monopole and dipole removed after masking. This mask has $f_{\text{sky}} = 0.78$, slightly larger than used in previous studies (Copi et al. 2013a). Though this shifts the calculated cut-sky $S_{1/2}$ to a larger value, and thus to a larger p -value, here we are only interested in the relative contributions due to early-time and late-time correlations, not the absolute value.

3.2 Realizations

Our analyses are based on sets of realizations generated from different choices of the total $a_{\ell m}$. From these total $a_{\ell m}$, pairs of early-time, $a_{\ell m}^e$, and late-time, $a_{\ell m}^l$, contributions were generated as discussed in App. A. The sets of realizations are as follows.

(i) A total of 200 000 realizations of $a_{\ell m}$ drawn from the best-fitting Λ CDM model were generated. For each realization, a single pair of the $a_{\ell m}^e$ and $a_{\ell m}^l$ were subsequently generated. This set of realizations represents the expected distribution from Λ CDM and predominantly contains skies

with large $S_{1/2}$. We refer to this set as the *unconditioned- Λ CDM* realizations.

(ii) The $a_{\ell m}$ were extracted from each of the cleaned, full-sky *Planck* Release-2 maps (SMICA, Commander, SEVEM, and NILC). A set of realizations of pairs of $a_{\ell m}^e$ and $a_{\ell m}^l$ were generated for each map. Since each of the four Release-2 maps produced nearly identical results, only those from the SMICA map will be discussed in detail. This SMICA set again contains 200 000 realizations. We refer to this set as the *SMICA-conditioned* realizations.

(iii) Ten realizations of $a_{\ell m}$ drawn from the best-fitting Λ CDM model constrained to have $S_{1/2} \approx S_{1/2}(\text{SMICA})$ were generated. For each of these ten low- $S_{1/2}$ realizations, 10 000 pairs of $a_{\ell m}^e$ and $a_{\ell m}^l$ were subsequently generated. This set of realizations represents Λ CDM skies with large-angle properties similar to those found in the SMICA map. It provides a check of whether the *SMICA-conditioned* set was typical or atypical among low $S_{1/2}$ Λ CDM realizations. We refer to these sets collectively as the *low- $S_{1/2}$ - Λ CDM* realizations.

(iv) Subsets from the *unconditioned- Λ CDM* realizations were selected with $S_{1/2}(ee, ee) \leq S_{1/2}^{\text{max}}(ee, ee)$, for a variety of values of $S_{1/2}^{\text{max}}(ee, ee)$. In addition, in order to probe very small values of $S_{1/2}(ee, ee)$, the *unconditioned- Λ CDM* realizations were augmented by creating additional realizations with $S_{1/2}(ee, ee)$ as low as $500 \mu\text{K}^4$. This set of realizations allowed us to probe the effect of suppressed early-time correlations in the context of Λ CDM. Note that this does not represent a physical model for the suppression of early-time correlations. No physics has been put in to cause the suppression. It represents the effect of the ℓ ISW on $S_{1/2}$ in the (near) absence of early-time contributions. We refer to these sets collectively as the *low- $S_{1/2}(ee, ee)$ - Λ CDM* realizations.

4 RESULTS

To begin, we first compare the *unconditioned- Λ CDM* to the *SMICA-conditioned* realizations. The upper-left panel of Fig. 1 shows the $S_{1/2}$ probability distribution function (PDF) for the *unconditioned- Λ CDM* realizations. Here the $S_{1/2}$ value for the SMICA map with the Common mask, $S_{1/2}(\text{SMICA}) = 2153 \mu\text{K}^4$, is shown as the vertical dashed line and has a p -value of 0.58 per cent, i.e. only that percentage of the *unconditioned- Λ CDM* realizations had a smaller $S_{1/2}$ than SMICA.

The remaining panels in Fig. 1 display the auto-correlated parts of $S_{1/2}$ for both the *unconditioned- Λ CDM* and the *SMICA-conditioned* realizations. The biggest difference between the two is that $S_{1/2}(ee, ee)$ is noticeably suppressed in the *SMICA-conditioned* realizations compared to the *unconditioned- Λ CDM* ones. This is in part because $S_{1/2}(ee, ee)$ is the largest single contribution to $S_{1/2}$; however, note that in the *SMICA-conditioned* realizations, the mean of the PDF of $S_{1/2}(ee, ee)$ is shifted *below* that of $S_{1/2}(el, el)$. The latter is barely affected, and perhaps even slightly *increased* compared to the *unconditioned- Λ CDM* realizations. Meanwhile the $S_{1/2}(ll, ll)$ PDF is only slightly changed and, more suggestively, if the SMICA value (vertical line) were pure $S_{1/2}(ll, ll)$, that value would be unremarkable.

These results taken together begin to suggest that the

¹ See <http://healpix.sourceforge.net> for more information.

² See <http://camb.info/> for information and access to the code.

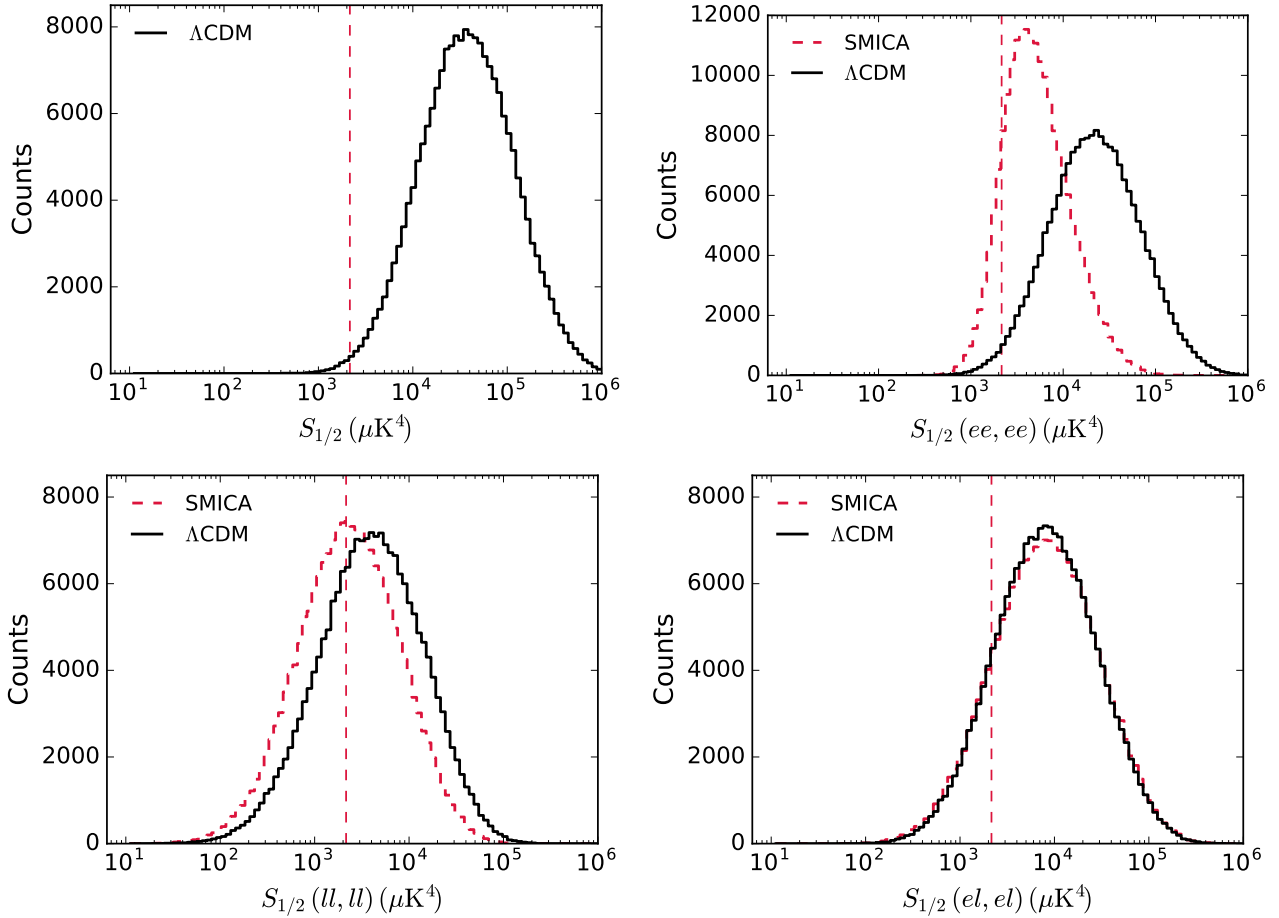


Figure 1. Distributions of masked-sky $S_{1/2}$ from 200 000 *unconditioned- Λ CDM* realizations (solid, black lines) and *SMICA-conditioned* realizations (dashed, red lines). (For detailed descriptions of the realizations, see section 3.2.) The vertical lines represent the observed value of the masked-sky $S_{1/2}$ from the SMICA map. Top left: The total $S_{1/2}$ probability distribution function (PDF) which includes contributions from SW, eISW, and ℓ ISW. The SMICA map has a single value so is only represented by the vertical line in this panel. Top right: The PDF of the auto-correlated, pure-early contribution, $S_{1/2}(ee, ee)$, which shows a suppression in the *SMICA-conditioned* realizations compared to the *unconditioned- Λ CDM* ones. Bottom left: The PDF of $S_{1/2}(ll, ll)$ which shows little change from the *unconditioned- Λ CDM* realizations to the *SMICA-conditioned* ones – both distributions are consistent with the observed SMICA value, i.e. the observed $S_{1/2}$ value would not be anomalous in a ℓ ISW-only sky. Bottom right: The PDF of $S_{1/2}(el, el)$ which is nearly identical in both the *unconditioned- Λ CDM* realizations and the *SMICA-conditioned* ones.

observed $S_{1/2}$ value is consistent with, and perhaps indicative of, a suppression of early-time correlations. If one could simply turn off early-time effects in the theory without changing the late-time effect (e.g. somehow set $C^{ee}(\theta) = 0$ with C^{ee} having the obvious meaning of replacing C_ℓ in (2) with C_ℓ^{ee}), so that the final $S_{1/2}$ distribution would be completely $S_{1/2}(ll, ll)$, then the observed SMICA $S_{1/2}$ value would lie close to the mean of the PDF.

To understand how the rare, small- $S_{1/2}$ realizations of Λ CDM are produced we consider the correlation between pairs of $S_{1/2}(X, Y)$. Fig. 2 shows a scatter-plot of the ‘mixed’ parts with the ‘auto’ parts of $S_{1/2}$. Here

$$S_{1/2}(\text{mixed}) \equiv (S_{1/2}(ee, ll) + S_{1/2}(ee, el) + S_{1/2}(ll, el)) \quad (10)$$

and

$$S_{1/2}(\text{auto}) \equiv S_{1/2}(ee, ee) + S_{1/2}(ll, ll) + S_{1/2}(el, el). \quad (11)$$

In the left panel, we see that in the *unconditioned- Λ CDM* realizations there are roughly equal numbers of positive

and negative values of the mixed component, while for the *SMICA-conditioned* ones (right panel) there is an almost complete suppression of the positive values, supplemented by an almost perfect anti-correlation between $S_{1/2}(\text{mixed})$ and $S_{1/2}(\text{auto})$. Thus, the combination of these two nearly cancel producing a small $S_{1/2}$.

The *low- $S_{1/2}$ - Λ CDM* realizations allow us to determine whether the usual method of producing a small $S_{1/2}$ found in the *SMICA-conditioned* realizations (the significant cancellation) is typical in realizations of Λ CDM with small $S_{1/2}$. From the *low- $S_{1/2}$ - Λ CDM* realizations, we found the same anti-correlation between $S_{1/2}(\text{mixed})$ and $S_{1/2}(\text{auto})$ thus showing that if the observed low $S_{1/2}$ is due to a fluke in Λ CDM, it may at least be a ‘typical fluke’.

Finally, Fig. 3 shows the p -value of the SMICA $S_{1/2}$ value among the *low- $S_{1/2}(ee, ee)$ - Λ CDM* realization as a function of the upper limit on $S_{1/2}(ee, ee)$. A suggestive interpolation between the lowest $S_{1/2}^{\text{max}}(ee, ee)$ in the *low- $S_{1/2}(ee, ee)$ - Λ CDM* realizations ($500 \mu\text{K}^4$, the lowest value

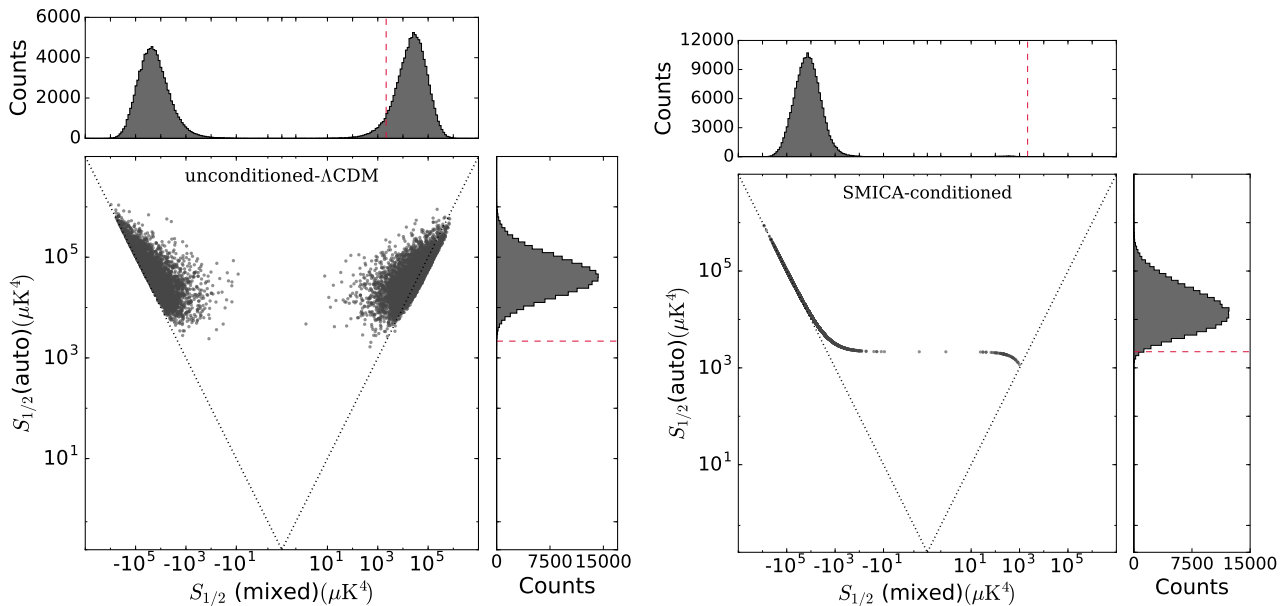


Figure 2. Scatter plots of masked-sky $S_{1/2}(\text{mixed})$ versus $S_{1/2}(\text{auto})$, as defined in Eqs. (10) and (11), for the *unconditioned- Λ CDM* realizations (left) and for the *SMICA-conditioned* realizations (right). For reference, the dotted lines show $S_{1/2}(\text{mixed}) = \pm S_{1/2}(\text{auto})$, while red-dashed lines correspond to the observed masked-sky $S_{1/2}$ value from the SMICA map. For the *unconditioned- Λ CDM* realizations we see roughly equal numbers of positive and negative values of $S_{1/2}(\text{mixed})$. In contrast, for the *SMICA-conditioned* realizations there is an almost complete suppression of the positive values of $S_{1/2}(\text{mixed})$, and an almost perfect anti-correlation between $S_{1/2}(\text{mixed})$ and $S_{1/2}(\text{auto})$. These two combine to yield the observed small value of $S_{1/2}$. Note that Λ CDM realizations constrained by a small $S_{1/2}$ sky (the *low- $S_{1/2}$ - Λ CDM* realizations) consistently exhibit the same feature (not shown).

for which a sufficient number of realizations was generated) and $S_{1/2}(ee, ee) = 0$ (as deduced from the $S_{1/2}(ll, ll)$ distribution from the *unconditioned- Λ CDM* realizations, see the bottom left panel of Fig. 1) is shown as a dotted curve. We see that whereas the SMICA value is rare (p -value of 0.58 per cent) among generic Λ CDM skies, it is reasonably common ($p > 10$ per cent) when $S_{1/2}(ee, ee)$ is sufficiently small, approaching $p \approx 32$ per cent at $S_{1/2}^{\text{max}}(ee, ee) = 0$. Because the *Planck* Release-2 SMICA value of $S_{1/2}$ (with the *Common* mask) is somewhat larger than that found in earlier maps, we have confirmed that the same statement holds true even if we demand that $S_{1/2} < 1600 \mu\text{K}^4$ (a value more typical of *WMAP* and *Planck* Release-1 maps and masks). This strongly suggests that non-fluke explanations of the observed low values of $S_{1/2}$ could reasonably expect to arise from new physics at or near the LSS, without undue concern that the ℓ ISW contribution would spoil the explanation, though of course that would need to be checked in any specific proposed model.

5 CONCLUSIONS

Using the *Planck* Release-2 SMICA, Commander, SEVEM and NILC synthetic full-sky maps, and the best-fitting *Planck* (TT + lowP + lensing) parameters (Planck Collaboration et al. 2015b), we have created sets of realizations of the CMB temperature with the contributions from early-time and late-time physics separated. The early-time physics is represented through the Sachs-Wolfe and early-time integrated Sachs-Wolfe effects, whereas the late-time physics is represented through the late-time integrated Sachs-Wolfe effect.

For each generated sky we have calculated, using the *Planck* Release-2 Common (UT78) mask, the angular auto-correlation functions for the early-time and late-time contributions, $\mathcal{C}^{ee}(\theta)$ and $\mathcal{C}^{ll}(\theta)$, and the cross-correlation function $\mathcal{C}^{el}(\theta)$. These have then been combined into the six contributions to $S_{1/2}$, the statistic that characterizes large-angle correlations of the CMB temperature, giving the auto-correlation contributions $S_{1/2}(ee, ee)$, $S_{1/2}(el, el)$, and $S_{1/2}(ll, ll)$, and the mixed-correlation contributions $S_{1/2}(ee, el)$, $S_{1/2}(ee, ll)$, and $S_{1/2}(el, ll)$. Finally, for these $S_{1/2}(X, Y)$ we have produced probability distribution functions (PDFs).

Examining these PDFs we find that in Λ CDM low values of cut-sky $S_{1/2}$, such as are inferred from the *Planck* Release-2 full-sky maps, typically occur when, by chance, $S_{1/2}(ee, ee)$ is somewhat suppressed, and the remaining auto-correlations are cancelled by the mixed-correlations. In other words, Λ CDM realizations with low $S_{1/2}$ typically *do not have* very low $S_{1/2}(ee, ee)$, instead, they also include chance cancellations. The late-time contribution, $S_{1/2}(ll, ll)$, need not be suppressed, suggesting that there is no reason to expect unusually low amplitudes of late-time ISW, given the low observed value of $S_{1/2}$.

Alternatively, when we examine Λ CDM realizations in which $S_{1/2}(ee, ee)$ is *constrained* to be suppressed well below the value of $S_{1/2}$ inferred from the *Planck* Release-2 full-sky maps, we find that the inferred *Planck* value of $S_{1/2}$ is no longer anomalous. This suggests that physical explanations that operate to suppress correlations on the last scattering surface (i.e. at high redshifts), may be successful, in that they need not be spoiled by the ℓ ISW effect. There is thus no obvious need to (anti-)correlate early and late-time physics

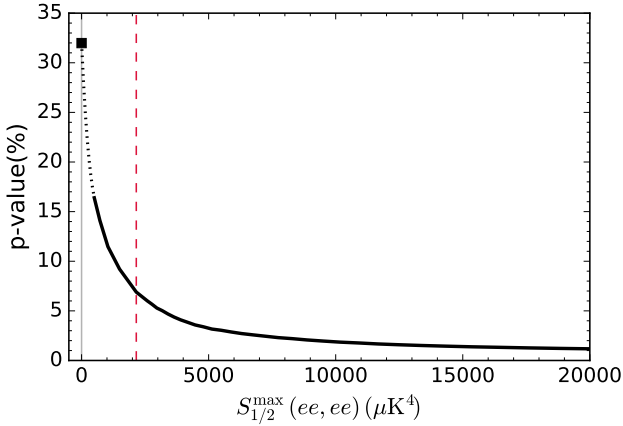


Figure 3. p -value of $S_{1/2} < S_{1/2}(\text{SMICA}) = 2153 \mu\text{K}^4$ among realizations of ΛCDM with $S_{1/2}(ee, ee) < S_{1/2}^{\text{max}}(ee, ee)$ as a function of that $S_{1/2}^{\text{max}}(ee, ee)$ (solid line), derived from the low - $S_{1/2}(ee, ee)$ - ΛCDM realizations. The small p -value of $S_{1/2}$ in the $unconditioned$ - ΛCDM realizations, 0.58 per cent, is recovered at large $S_{1/2}^{\text{max}}(ee, ee)$, while an unremarkable p -value is found as $S_{1/2}^{\text{max}}(ee, ee) \rightarrow 0$. When $S_{1/2}^{\text{max}}(ee, ee) = 0$, the p -value is that of a purely ℓISW sky, ie. approximately 32 per cent. The dotted curve is a suggestive interpolation between the p -values for $S_{1/2}^{\text{max}}(ee, ee) = 0$ and $S_{1/2}^{\text{max}}(ee, ee) = 500 \mu\text{K}^4$. The red dashed line marks $S_{1/2}(\text{SMICA})$.

provided that the late-time physics remains similar to that in the ΛCDM model.

ACKNOWLEDGEMENTS

GDS and MO’D are partially supported by Department of Energy grant DE-SC0009946 to the particle astrophysics theory group at CWRU. MO’D is partially supported by the CAPES Foundation of the Ministry of Education of Brazil. Some of the results in this paper have been derived using the HEALPIX (Górski et al. 2005) package.

REFERENCES

- Bennett C. L., et al., 2011, *ApJS*, **192**, 17
 Copi C. J., Huterer D., Schwarz D. J., Starkman G. D., 2006, *MNRAS*, **367**, 79
 Copi C. J., Huterer D., Schwarz D. J., Starkman G. D., 2007, *Phys. Rev. D*, **75**, 023507
 Copi C. J., Huterer D., Schwarz D. J., Starkman G. D., 2009, *Mon. Not. Roy. Astron. Soc.*, **399**, 295
 Copi C. J., Huterer D., Schwarz D. J., Starkman G. D., 2010, *Advances in Astronomy*, **2010**, 847541
 Copi C. J., Huterer D., Schwarz D. J., Starkman G. D., 2013a, preprint, ([arXiv:1310.3831](https://arxiv.org/abs/1310.3831))
 Copi C. J., Huterer D., Schwarz D. J., Starkman G. D., 2013b, *MNRAS*, **434**, 3590
 Dvorkin C., Peiris H. V., Hu W., 2008, *Phys. Rev. D*, **77**, 063008
 Górski K. M., Hivon E., Banday A. J., Wandelt B. D., Hansen F. K., Reinecke M., Bartelmann M., 2005, *ApJ*, **622**, 759
 Hajian A., 2007, ArXiv Astrophysics e-prints,

- Hinshaw G., Branday A. J., Bennett C. L., Gorski K. M., Kogut A., Lineweaver C. H., Smoot G. F., Wright E. L., 1996, *ApJ*, **464**, L25
 Lewis A., Challinor A., Lasenby A., 2000, *ApJ*, **538**, 473
 Planck Collaboration et al., 2015b, preprint, ([arXiv:1502.01589](https://arxiv.org/abs/1502.01589))
 Planck Collaboration et al., 2015a, preprint, ([arXiv:1506.07135](https://arxiv.org/abs/1506.07135))
 Schwarz D. J., Copi C. J., Huterer D., Starkman G. D., 2015, preprint, ([arXiv:1510.07929](https://arxiv.org/abs/1510.07929))
 Spergel D. N., et al., 2003, *ApJS*, **148**, 175
 Yoho A., Copi C. J., Starkman G. D., Kosowsky A., 2014, *MNRAS*, **442**, 2392
 Yoho A., Aiola S., Copi C. J., Kosowsky A., Starkman G. D., 2015, *Phys. Rev. D*, **91**, 123504

APPENDIX A: CONSTRAINED REALIZATIONS

Generating constrained, correlated Gaussian random variables is a well-known topic. Here we apply the standard approach to generating pairs of early-time and late-time skies from a given total sky. This discussion is based closely on Appendix A of Copi et al. (2013b).

In ΛCDM , the temperature anisotropies from early-time and late-time physics, $a_{\ell m}^e$ and $a_{\ell m}^l$, respectively, are correlated and related to the associated full-sky anisotropies, $a_{\ell m} = a_{\ell m}^e + a_{\ell m}^l$. Thus, given the full-sky $a_{\ell m}$ and the power spectra, C_ℓ , C_ℓ^e , and C_ℓ^l , the correlated pairs, $a_{\ell m}^e$ and $a_{\ell m}^l$, can be generated.

Though typically written in terms of a complex basis, so that the $a_{\ell m}$ are complex coefficients, it is more convenient to work in a real basis when generating realizations. Let a_j represent a (real) coefficient in the real basis. The index j refers to the pair of standard spherical-harmonic indices (ℓ, m) , and takes values 0 to 2ℓ , for each ℓ . The complex coefficients are constructed from the real coefficients as

$$a_{\ell m} = \begin{cases} a_0, & m = 0 \\ \frac{1}{\sqrt{2}} (a_{2m-1} + i a_{2m}), & m > 0 \end{cases} \quad (\text{A1})$$

Unconstrained realizations of ΛCDM can then be generated in the real basis as

$$a_j = \sqrt{C_\ell} \zeta_1, \quad (\text{A2})$$

$$a_j^l = \frac{C_\ell^e + C_\ell^l}{\sqrt{C_\ell}} \zeta_1 + \sqrt{C_\ell^l - \frac{(C_\ell^e + C_\ell^l)^2}{C_\ell}} \zeta_2, \quad (\text{A3})$$

where ζ_1 and ζ_2 are independent Gaussian random variables each drawn from a distribution with zero mean and unit variance.

However, once the full-sky $a_{\ell m}$ are determined from observations the $a_{\ell m}^l$ (or any other correlated quantity) is partially constrained. Given particular values for the $a_{\ell m}$ we need to generate realizations of $a_{\ell m}^l$ that are consistent with these inputs. In other words, instead of randomly drawing a number for ζ_1 when generating $a_{\ell m}^l$, we instead *solve* for ζ_1 from Eq. (A2). This amounts to rewriting Eq. (A3) as

$$a_j^l = \frac{C_\ell^e + C_\ell^l}{C_\ell} a_j + \sqrt{C_\ell^l - \frac{(C_\ell^e + C_\ell^l)^2}{C_\ell}} \zeta_2, \quad (\text{A4})$$

where ζ_2 is still to be a random draw from a normal distribution. Finally, for each draw, the early sky coefficients are obtained by the difference $a_{\ell m}^e = a_{\ell m} - a_{\ell m}^l$.

This paper has been typeset from a \TeX/L\AA\TeX file prepared by the author.